# An *OpIE2*-DsRed marker disrupts female blood-feeding and shortens lifespan in the malaria vector *Anopheles gambiae*

Arad Sarig[1], Evyatar Sar-Shalom[1], Ebrima SM Kolley[1], Elad Shmuel Yonah[1], Lee Benjamin Lamdan[1], Ariel Roselin Lewin[1], Tamir Partosh[2], Gur Pines[2], Jonathan D. Bohbot[1] and Philippos Aris Papathanos[1,3]

1. Department of Entomology, Institute of Environment Sciences, Robert H. Smith Faculty of Agriculture, Food and Environment, Hebrew University of Jerusalem, Rehovot, Israel
2. Institute of Plant Protection, Agricultural Research Organization - Volcani Institute, Rishon LeZion, Israel
3. Corresponding author: p.papathanos@mail.huji.ac.il

**Abstract**

*Anopheles gambiae* is one of the principle vectors of human malaria. Over the past two decades, transgenic mosquito strains have been instrumental for studying mosquito biology and developing genetic control strategies such as gene drives. Mosquito transformants are typically identified using fluorescent markers which are assumed to be phenotypically neutral. While generating CRISPR-based gene drive strains with an *OpIE2*-DsRed marker we unexpectedly found that transgenic females were unable to blood-feed and were consequently sterile. Males, in contrast, appeared physiologically normal and fertile and enabled maintenance of the strains. Recognizing the potential utility of dominant, female-specific sterility for mosquito control, we established new strains controlling for transgene content and integration site, which confirmed that the specific *OpIE2*-DsRed marker was directly responsible for the blood-feeding defect. Behavioral assays showed that females exhibited normal attraction to a membrane feeder but failed to initiate blood-feeding, performing repeated cycles of probing and proboscis grooming in rapid succession before ultimately leaving the feeder unfed. Microscopic examination of *OpIE2a* females revealed a pronounced curvature of the proboscis. Similar malformations were also present in males and likely contributed to their reduced adult lifespan, overturning our preliminary conclusion of normal male fitness. A second promoter variant (*OpIE2b*), differing in flanking sequences at the IE-2 junction, drove bright marker expression without impairing blood-feeding or survival when integrated at the same genomic site. These findings demonstrate how minor differences in promoter architecture can elicit major, unexpected phenotypes. *OpIE2b*

provides a robust, phenotypically neutral marker for *An. gambiae* research, while *OpIE2a* highlights the need for rigorous validation of transgenic components intended for research and applied releases.

## Introduction

The African malaria mosquito *Anopheles gambiae* is among the most efficient vectors of *Plasmodium* parasites and remains a major public-health challenge in sub-Saharan Africa.. Transmission occurs exclusively through the blood-feeding of adult females, which digest blood to obtain nutrients required for oocyte development and egg production. This link between blood-feeding and reproduction makes female feeding behavior a critical determinant of both the vectorial capacity and mosquito population dynamics.

Since stable germline transformation of *Anopheles* mosquitoes was first demonstrated in the early 2000s (Catteruccia et al., 2000; Grossman et al., 2001), transgenic strains have become important tools for mosquito research. They now underpin a wide range of studies in mosquito biology, from malaria transmission biology (Pascini et al., 2022) to olfaction and sensory behavior (Riabinina et al., 2016; Maguire et al., 2022; Georgiades et al., 2023; Giraldo et al., 2024) and insecticide resistance (Adolfi et al., 2019). Transgenic approaches are also integral to the development of genetic control strategies, including gene drives designed for population suppression and replacement (Kyrou *et al.*, 2018; Carballar-Lejarazú *et al.*, 2020; Haber *et al.*, 2024; Li *et al.*, 2025; Strampelli *et al.*, 2025; Tolosana *et al.*, 2025; Verkuijl *et al.*, 2025).

These advances depend not only on the ability to introduce and stably integrate transgenes into the mosquito genome, but also on reliably identifying transformed individuals. In practice, this is achieved through fluorescent reporters driven by 5’ and 3’ regulatory sequences (hereafter 5’ regulatory sequences are referred to as promoters for simplicity) that ensure strong and easily detectable expression, most often during larval stages when screening is performed under a fluorescent microscope. An ideal reporter is bright throughout development, spectrally distinct from other markers (e.g., eGFP vs DsRed), and compatible with multiple constructs, for instance through tissue-specific expression patterns (e.g., eye- versus muscle-specific). Differences in brightness between homozygotes and heterozygotes can sometimes aid husbandry and genetics, though these are highly dependent on the genome integration site and are more reliably distinguished using automated optical sorters (e.g., COPAS) than by eye

(Marois, 2024). Above all, reporters should be phenotypically neutral, imposing no measurable fitness costs that might confound experiments or limit their application.

The most widely used marker in *An. gambiae* is the synthetic *3xP3* promoter which drives strong neuron- and eye-specific fluorescence (Berghammer, Klingler and Wimmer, 1999). The heterologous *Actin5C* promoter from *Drosophila melanogaster* (Volohonsky *et al.*, 2015), though considerably longer, yields broad somatic expression in mosquito larvae and is frequently paired with *3xP3* markers in dual-reporter constructs or crosses for improved sorting and multiplexing (Catteruccia, Benton and Crisanti, 2005). Endogenous promoters such as the *polyubiquitin* promoter (Adolfi *et al.*, 2018), which drives broad multi-tissue expression, and the *α-tubulin-1b* promoter (Lycett, Amenya and Lynd, 2012), which directs consistent neuronal and testis expression with insertion-dependent activity in other tissues, have also been demonstrated, but remain restricted to their original reports and have not yet seen wider adoption. In addition, viral promoters such as *hr5-IE1*, derived from baculoviruses, have been used to drive strong, ubiquitous marker expression in transgenic *An. gambiae* (Grossman *et al.*, 2001; Meredith *et al.*, 2013). However, beyond *hr5-IE1*, the use of viral promoters in this species remains largely underexplored, despite their popularity in insect cell culture and other insect systems.

One such element, the *OpIE2* promoter, originates from the immediate early gene 2 (*IE-2*) of the *Orgyia pseudotsugata* multicapsid nucleopolyhedrovirus (OpMNPV) (Theilmann and Stewart, 1992). It has been widely adopted in lepidopteran and dipteran cell line transfections, where it drives high and constitutive expression of transgenes (Pfeifer *et al.*, 1997; Xu *et al.*, 2013). *In vivo*, the *OpIE2* promoter has been incorporated into transgenic constructs in several insect species, including in *Drosophila melanogaster* (Buchman *et al.*, 2018; Kandul *et al.*, 2019), *Drosophila suzuki* (Liu *et al.*, 2025; Witherbee and Gamez, 2025), *Bombyx mori* (Li *et al.*, 2015; Tang *et al.*, 2018), *Pectinophora gossypiella* (Simmons *et al.*, 2011)*, Plutella xylostella* (Martins *et al.*, 2012)*, Ceratitis Capitata* (Davydova *et al.*, 2023) and multiple mosquitoes, including *Aedes aegypti* (Li *et al.*, 2017; Estevez-Castro *et al.*, 2024; Rouyar *et al.*, 2024; Vainer *et al.*, 2024) *Aedes albopictus* (Lutrat *et al.*, 2022; Zaada *et al.*, 2025), *Culex quinquefasciatus* (Feng *et al.*, 2021) where it consistently provides strong expression. In *An. gambiae*, however, use of *OpIE2* has been more limited, with one study reporting its application to drive expression of a puromycin resistance gene for antibiotic selection of transgenic larvae (Volohonsky *et al.*, 2015).

Here, we report that expression of DsRed in *An. gambiae* under a specific variant of the *OpIE2* promoter severely impairs female blood-feeding and reduces male longevity. To investigate this effect, we generated a number of strains controlling for genomic integration site and construct elements, characterized female feeding behavior, and tested an alternative *OpIE2* promoter sequence. The alternative promoter maintained marker visibility while restoring normal feeding, underscoring that promoter choice can have profound effects on mosquito biology and is critical for both transgenic tool design and genetic control strategies.

## Results

### Generation of *OpIE2*-DsRed transgenic strains

In previous work, we used an *OpIE2*-DsRed fluorescent marker in *D. melanogaster* strains containing split Cas9 and gRNA sex ratio distorters (Haber et al., 2024). Seeking to develop similar capacities in *An. gambiae*, we cloned this *OpIE2*-DsRed to label sgRNA transgenic constructs, complementing available Cas9 strains marked by fluorescent proteins driven by the neuron-specific *3xP3* promoter. Four transformation constructs were generated, each containing *OpIE2*-DsRed and single *U6*-driven sgRNA targeting different sex chromosome sequences (**Figure 1A**). The constructs included *piggyBac* repeats for transposase-mediated integration and an *attB* site for □*C31*-mediated site-specific recombination. Constructs were injected either into wild type eggs with a *piggyBac* transposase helper or into eggs of the *attP*-E strain, which carries a well-characterized, *3xP3*-CFP-labelled *attP* docking site on chromosome 3 (Meredith *et al.*, 2011). In total, eight independent strains were generated, four with random piggyBac insertion (construct #1) and three in the *attP*-E line (constructs #2-4; **Supplementary Table 1**).

Larvae of all strains displayed bright DsRed fluorescence in thoracic and abdominal segments, and weaker expression in the larval head (**Figure 1B**). In pupae, DsRed fluorescence was bright throughout the entire body (**Figure 1B**). However, adult transgenic females from all eight lines failed to blood-feed, and no eggs were produced when oviposition bowls were provided 48 hours after feeding. In contrast, transgenic males appeared physiologically normal and fertile, producing offspring when crossed to wild-type females and enabling maintenance of the strains as heterozygotes. Because the defect was consistent across both *piggyBac* and □*C31* integrations, we concluded that it likely resulted from the *OpIE2*-DsRed cassette itself rather than the insertion site or sgRNA sequence, which differed between constructs.

To test this, we generated new constructs in which DsRed was driven by the *Actin5C* promoter instead of *OpIE2*. When integrated at the same *attP-E* site, these constructs restored female blood-feeding, suggesting that the phenotype was specific to *OpIE2*-DsRed expression (**Figure 1A**). We confirmed this by generating a new construct containing only the *OpIE2*-DsRed cassette and integrating it into the *attP*-E site. As this strain exhibited the same non-blood-feeding phenotype, we concluded that *OpIE2*-DsRed expression alone was sufficient to interrupt female blood-feeding.

When we analyzed the cloned *OpIE2* promoter sequence, we noticed that the promoter derived from the *Drosophila* constructs differed from another *OpIE2* promoter that we recently used in *Aedes albopictus* (Zaada *et al.*, 2025). To better understand these differences we aligned both promoters, which we called *OpIE2a* (for *D. melanogaster* constructs) and *OpIE2b* (for *A. albopictus* constructs) to the *OpMNPV IE-2* gene region. Both promoters shared a 461 bp core sequence, but there were several differences in the cloned flanking sequences. (**Figure 1C**). The *OpIE2a* promoter extended 66 bp into the viral *IE-2* coding sequence, including the start codon and fusing 22 amino acids of *IE-2* to the N-terminus of DsRed. The *OpIE2b* promoter included an additional 90 bp upstream sequence, but terminated prior to the *IE-2* start codon in its 3' end, where it connects to DsRed. The 3' end of the *OpIE2b* promoter also contained *T7* and *EM7* expression elements and restriction sites retained from previous cloning steps.

To test whether these sequence differences accounted for the phenotype, we generated a new strain carrying the *OpIE2b*-DsRed cassette integrated into the same *attP-E* site (**Figure 1A**). DsRed expression driven by *OpIE2b* was slightly weaker in larvae, pupae and adults compared to *OpIE2a* but followed a similar spatial pattern (**Figure 1C**). Importantly, *OpIE2b*-DsRed females blood-fed normally, demonstrating that *OpIE2a*-DsRed caused the feeding defect.

**Blood-feeding capacity is impaired in *OpIE2a-DsRed* females.**

To characterize and quantify the blood-feeding defect, we established triplicate cages of 14-20 *OpIE2a*-DsRed or *OpIE2b*-DsRed females, previously mated to wild type males, alongside wild type control females. Females were offered a membrane feeder containing bovine blood for 25 minutes, and a camera inside each cage recorded female behavior (**Figure 2A**). At the end of the assay, all females were aspirated from their cages to record the number of blood-fed females. *OpIE2b*-DsRed females fed normally, with feeding rates indistinguishable from wild

type females ($p$ = 0.254, unpaired two-sided $t$-test; **Figure 2B**). In contrast, none of the *OpIE2a*-DsRed females fed during the 25 minute window ($p$ = 0.0002, unpaired two-sided $t$-test; **Figure 2B**). To test whether additional stimulation could elicit feeding, *OpIE2a*-DsRed females were given a 15-minute rest and re-offered fresh blood for an additional 30 minutes, accompanied by intermittent human breath stimulation to mimic host-associated cues. Eventually a small fraction of *OpIE2a*-DsRed females managed to feed (median = 6.25%;  four females across all replicates; **Figure 2C**).

Recordings of female blood-feeding behavior were analysed using a trained behavioral detection and classification neural network built on the YOLOv11 object detector (Khanam and Hussain, 2024) and adapted from Vainer et al. (2024). Feeder occupancy (number of females detected per minute) was analyzed using a linear mixed model with strain and time as fixed effects and replicate as a random intercept. *OpIE2a*-DsRed females showed a significantly steeper decline in feeder visits over time compared to wild-type controls (interaction $\beta$ = –0.158 ± 0.038 SE, $p$ < 0.001), whereas *OpIE2b*-DsRed females did not differ significantly ($\beta$ = –0.047 ± 0.038 SE, $p$ = 0.21). At the beginning of the assay (time = 0), *OpIE2a*-DsRed females already exhibited fewer visits than wild type (–6.66 ± 2.23 SE, $p$ = 0.0028), while *OpIE2b*-DsRed females were comparable to controls ($p$ = 0.08; **Figure 2D**).

Behavioral ethograms for the first five minutes of each assay were also manually generated, annotating arrival, probing, blood-feeding and departure events for each female (**Figure 2E**). Wild type and *OpIE2b*-females began probing shortly after arrival on the feeder and remained stationary once feeding began. In contrast, *OpIE2a*-DsRed females exhibited normal attraction to the feeder but failed to initiate blood-feeding, performing repeated cycles of probing and proboscis grooming in rapid succession before ultimately leaving the feeder unfed (**Figure 2E**). These observations indicate that the *OpIE2a*-DsRed defect affects feeding initiation rather than attraction.

### ***OpIE2a*-DsRed adults exhibit a curved proboscis**

To investigate whether the behavioral defect corresponded to morphological abnormalities, we examined adult mouthparts by stereofluorescence microscopy. All *OpIE2a*-DsRed females displayed a pronounced distal curvature of the proboscis, in contrast to the straight proboscis observed in wild-type and *OpIE2b*-DsRed females (**Figure 3A-C)**. Because the feeding defect initially appeared female-specific, we also examined male mouthparts as controls (**Figure 3D-F)**. Unexpectedly, *OpIE2a*-DsRed males exhibited the same deformity, with proboscis curvature

even more pronounced than in females, whereas *OpIE2b*-DsRed males retained normal proboscis morphology.

Fluorescence imaging revealed notable DsRed signals within the proboscis of *OpIE2a*-DsRed adults, but not in *OpIE2b*-DsRed mosquitoes imaged under identical exposure settings. The co-occurrence of proboscis-localized DsRed expression and curvature in *OpIE2a*-DsRed individuals suggests that promoter sequences influence expression in mouthpart tissues, coinciding with the observed morphological abnormalities.

### ***OpIE2a*-DsRed males exhibit reduced adult longevity**

To determine whether the *OpIE2a*-DsRed construct was associated with broader fitness costs, we assessed reproductive output and survival in both sexes. Among the few *OpIE2a*-DsRed females that successfully blood-fed after stimulation (n = 4), only two laid eggs. The number of eggs produced by these females was markedly lower than in controls, with a median of 28 eggs compared to 97.5 in wild-type and 74.5 in *OpIE2b*-DsRed females (unpaired two-sided *t*-test, $p = 0.042$; **Figure 4A**). In contrast, egg hatching rates did not differ significantly among strains (**Figure 4B**), indicating that fertilization and embryonic development were unaffected. When the blood-feeding assay was repeated with daughters of these females, none successfully blood-fed, confirming that the phenotype was heritable and fully penetrant (**Supplementary Table 2**).

To evaluate potential effects on male fitness, we crossed transgenic males from each strain to wild-type females, with wild-type intercrosses as controls. Egg hatching, larval-to-pupal, and pupal-to-adult survival rates were comparable across all groups (unpaired two-sided *t*-tests, all $p > 0.05$; **Figure 4C–E**), and adult sex ratios did not differ significantly (**Figure 4F**). However, adult longevity was severely reduced in *OpIE2a*-DsRed males, which had a median lifespan of only 6 days compared to 30 days in wild-type males (log-rank test, $p < 0.001$; **Figure 4G**). *OpIE2b*-DsRed males showed no difference in survival relative to controls (median 25 days vs 30 days, $p = 0.355$). Among females, *OpIE2a*-DsRed also exhibited a modest reduction in survival (median 20 days vs 25 days in wild type, $p = 0.035$), whereas *OpIE2b*-DsRed females survived comparably to controls (median 28 days vs 25 days, $p = 0.165$, **Figure 4H**). Together, these results overturned our initial conclusion that the *OpIE2a*-DsRed marker negatively affected fitness in a female-specific manner, by being detrimental to adult longevity, particularly among males, whereas the *OpIE2b*-DsRed variant maintains normal fecundity, survival, and developmental progression.

## Discussion

In this study, we demonstrate that expression of the fluorescent marker DsRed under the control of a specific variant of the *OpIE2* promoter (*OpIE2a*) causes profound and unexpected phenotypic effects in *An. gambiae*. Females carrying the *OpIE2a*-DsRed marker were unable to blood-feed and were therefore sterile, while males exhibited markedly reduced adult lifespan. In contrast, an alternative promoter variant, which we called *OpIE2b*, drove robust marker expression without measurable effects on feeding, development or longevity. These results reveal that even minor differences in promoter architecture can produce major biological consequences, emphasizing the need to validate commonly used regulatory elements when deployed in new species or experimental contexts.

The female blood-feeding impairment associated with *OpIE2a* was fully penetrant and heritable, persisting across generations - some lines are now over 30 generations old. Behavioral analyses showed that females were normally attracted to the feeder and initiated probing, but were unable to transition to sustained feeding. Microscopic examination identified a fully penetrant curvature of the proboscis in *OpIE2a* adults of both sexes, suggesting a structural rather than sensory or motivational basis for the defect. This distal bend likely prevents proper fascicle unsheathing and membrane penetration (Jones, 1978; Kong and Wu, 2010), explaining the repeated probing-grooming cycles and failure to feed. In males, the same curvature may interfere with sugar uptake, consistent with their severely shortened lifespan.

The difference between the *OpIE2a* and *OpIE2b* promoters lies in a 66-bp extension of *OpIE2a* into the viral *IE-2* coding region, which adds 22 amino acids fused to the N-terminus of DsRed. Although both variants contain the core regulatory motifs required for promoter activity (Theilmann and Stewart, 1992), this fusion likely alters the transcriptional or translation context, potentially modifying tissue specificity or protein localization. The presence of DsRed fluorescence within the proboscis of *OpIE2a* mosquitoes supports this hypothesis and suggests that local expression or toxicity in mouthparts underlies the morphological phenotype. While we did not directly measure promoter activity in dissected tissues or test other reporters under the same sequence, the data clearly demonstrate that even seemingly small differences in cloned promoter sequences can markedly change expression domains in transgenic insects, as we have previously observed a native germline promoter in transgenic *An. gambiae* strains (Papathanos *et al.*, 2009).

Beyond its mechanistic implications, this finding carries practical significance for transgenic mosquito research and genetic control tool development. First, transgenic reporters

are typically assumed to be phenotypically neutral (Catteruccia, Godfray and Crisanti, 2003; McArthur, Meredith and Eggleston, 2014); however as we have shown here, this assumption needs to be confirmed independently each time, since even standard markers can impose unexpected fitness costs when newly introduced into an engineered insect (Irvin *et al.*, 2004; Marrelli *et al.*, 2006).

In the case of *OpIE2a*-DsRed, the apparent female-specific sterility initially seemed attractive for engineering dominant female lethality, for example in self-limiting or split gene-drive systems (Champer *et al.*, 2022; Verkuijl *et al.*, 2025). However, the severe reduction in male longevity makes this configuration unsuitable for practical applications of population-suppression gene drives in its current form. If expression could be restricted to females, for example through the use of sex-specific splicing (Scali *et al.*, 2005; Fu *et al.*, 2010; Spinner *et al.*, 2022; Weng *et al.*, 2023, 2024; Liu, Rayes and Akbari, 2024), the dominant proboscis phenotype could be repurposed as a female-specific lethal trait in future designs.

Finally, the identification of *OpIE2b*-DsRed as a functionally neutral marker with bright, broad expression provides a valuable addition to the transgenesis toolkit available for *An. gambiae*. Because its expression pattern is distinct from commonly used markers such as *3xP3* or *Actin5C*, *OpIE2b* is well suited for multiplexed or combinatorial transgenic designs, including split gene drives and multi-color labeling systems.

In conclusion, our work reveals that promoter sequences alone can profoundly influence expression and phenotype in transgenic insects, transforming an otherwise inert fluorescent reporter into a dominant morphological impairment of mosquito physiology. This work offers both a cautionary example for construct design and a validated promoter variant (*OpIE2b*) suitable for future *An. gambiae* genetic engineering and gene-drive applications.

## Materials and methods

### Mosquito rearing

*An. gambiae* mosquitoes from the G3 (wild-type) strain, and all transgenic mosquito lines were reared under standard conditions of 28°C +/- 2°C and 80% +/- 10% relative humidity. Larvae were fed Essence fish food (Alltech Coppens), while adult mosquitoes were provided with a 10% (wt/vol) sucrose solution. For egg production, adult mosquitoes were allowed to mate for 5-7 days and then fed bovine blood using an artificial feeder (Hemotek, Ltd). An overnight egg-bowl was placed in the mosquito cages 48 hours post-blood-feeding for oviposition. Eggs were allowed 48 hours to hatch, and first instar larvae (L1) were transferred from the egg-bowl to

plastic trays, each containing approximately 250 larvae. The larvae were provided with ground fish food daily until they reached the pupal stage.

**Plasmid construction**

The *OpIE2*-DsRed transformation constructs were assembled using Golden-Gate assembly. Both plasmids contained an *OpIE2* promoter driving DsRed expression, differing only in the promoter variant used. The *OpIE2a* promoter fragment (541 bp) and the *OpIE2b* promoter fragment (652 bp) were PCR-amplified with primers incorporating BsaI recognition sites and compatible overhangs for directional assembly. Each promoter fragment was assembled upstream of the DsRed coding sequence to generate an *OpIE2*-DsRed cassette. In both constructs, the cassette was flanked by *piggyBac* inverted terminal repeats and a single *attB* site, enabling either random *piggyBac*-mediated or *φC31* site-specific integration. Final plasmids were validated by Oxford Nanopore sequencing (Plasmidsaurus) to confirm promoter sequence identity and integrity of the assembled cassette.

**Embryo microinjections**

Microinjections were performed into eggs of the *attP*-E strain, a homozygous transgenic line carrying an *attP* docking site on chromosome 3 and a *3xP3*-CFP fluorescence marker. *An. gambiae attP*-E eggs were gently aligned on a glass slide against a strip of thin nitrocellulose membrane, with moisture maintained using UltraPure™ Distilled Water (Invitrogen) applied to dampened filter paper. Using a fine brush, eggs were oriented with the posterior end facing upwards to maximize the chances of germline integration. A mixture of 300 ng/µl of the transformation construct and 100 ng/µl of a helper construct encoding vasa-driven *C31* integrase was injected. Hatched larvae were screened for transient expression of the *OpIE2*-DsRed marker, and all transient-positive and transgenic individuals were backcrossed to G3 wild-type mosquitoes. Progeny were maintained under standard rearing conditions.

**Blood-feeding assay and recording of female behavior**

Adult males and females were allowed to mate for 5–7 days prior to blood-feeding. For each strain, three biological replicates of 14–20 females were transferred to Bugdorm minicages (Model BD4S1515) for feeding. Females were offered blood for 25 min using the Hemotek Ltd membrane feeding system, with reservoirs filled with thawed bovine blood and sealed with stretched Parafilm. Feeding sessions were recorded using an Arducam camera system with

underlighting to document female behavior for subsequent analysis. Reservoirs were replaced with freshly thawed blood and new Parafilm membranes between assays performed on different strains. If no feeding was observed, a 15 min rest period was followed by a stimulation feeding session of 25 min, using the same Hemotek reservoir. During stimulation, air was exhaled intermittently onto the reservoir surface to increase female attraction. At the end of each assay, females were anesthetized at 4°C, and those with visibly blood-filled abdomens were aspirated and counted as successfully fed. Blood-feeding recordings were analyzed using a trained behavioral detection and classification neural network built on the YOLOv11 object detector (Khanam and Hussain, 2024), adapted from the behavioral analysis pipeline developed by Vainer et al. (2024). The pre-trained YOLOv11 model was tuned using a curated dataset of annotated images from our experimental setup, supplemented with external data to enhance detection robustness. Feeder occupancy was analyzed using a linear mixed model with the different strains and time as fixed effects and replicate as a random intercept.

Blood-feeding videos recorded during the assay were additionally analyzed using the open-source event-logging software BORIS - Behavioral Observation Research Interactive Software (Friard and Gamba, 2016). For each strain, one video with the highest number of females was selected for analysis (G3: 20 females, replicate R1; OpIE2b: 20 females, replicate R3; OpIE2a: 20 females, replicate R1; see **Supplementary Table 3**). Female behavior was tracked for the first 5 min following placement of the Hemotek feeder in the cage (time = 0). Because individual females could not be distinguished, behaviors were scored per visit to the feeder area. A visit was defined as entry into the area of interest over the Hemotek feeder, with multiple visits by the same female possible. For each visit, arrival and departure times, the number of probing events and, where applicable, the start and end times of blood-feeding were recorded.

**Female fertility assays**

Females that blood-fed during the assay were individually isolated for oviposition. The number of females per strain was determined by the number of *OpIE2a*-DsRed females that successfully fed after stimulation. Wild-type and *OpIE2b*-DsRed females were randomly selected to match this number. 48 h post blood-feeding, an egg-bowl was placed in each cage and removed the following day. Egg papers were photographed for counting using Clickmaster2000 (https://github.com/EuracBiomedicalResearch/clickmaster2000). Larvae were provided food 24 h after egg collection, and the number of hatched larvae was recorded 24 h

later to calculate hatching rates per female. Progeny from these assays were subsequently reared to adulthood and tested for blood-feeding behavior as described above (filming not performed due to technical limitations).

**Fitness and survival assays**

To evaluate potential fitness costs of the *OpIE2*-DsRed cassette, paternal crosses were established between transgenic males and wild-type females, with wild-type intercrosses as controls. Eggs were collected and counted to determine hatching rates. Hatchlings were distributed into trays at a density of 75 larvae per tray and reared under standard conditions. At pupation, male and female pupae were collected and counted. Pupae were allowed to emerge in Bugdorm minicages (Model BD4S1515), and the number of adults was determined by counting remaining pupal cases. These data were used to calculate larval-to-pupal and pupal-to-adult survival rates for each sex and strain, as well as the sex ratio of emerging adults.

Adult longevity was assessed in Bugdorm minicages (Model BD4S1515) containing 30–35 adults (24–72 h post-emergence) per strain, maintained on 10% sucrose solution. Dead adults were recorded and removed daily until all individuals had died. If sex or age at death could not be determined, the individual was censored on the day of discovery. Sucrose solution was replaced with a new, clean feeder every 14 days. Survival data were analyzed using Kaplan–Meier survival curves with log-rank tests.

**Mosquito imaging**

Photos of larvae, pupae, and adults were captured under standardized conditions to ensure consistent exposure across strains. Larvae at the fourth instar and pupae were imaged using an Olympus SZX16 binocular equipped with a U-HGLGPS fluorescence illumination system. All fluorescence images were acquired using identical exposure settings for each strain. Adult mosquitoes were imaged using a Nikon SMZ25 stereo microscope. 2-3 day old adults were first anesthetized with $CO_2$, after which legs and wings were removed to expose the body and proboscis for imaging. Dissected adults were then transferred to 50 mL plastic cups sealed with Parafilm containing silica gel desiccant to prevent condensation and placed at −20 °C for 30 min to achieve full immobilization. Following freezing, cups were thawed briefly at room temperature immediately before imaging. Fluorescence parameters and exposure settings were kept identical between strains to allow direct comparison of DsRed signal patterns.

## Statistical analysis

Statistical tests were performed in Python using standard packages (3.10.9; scipy 1.15.3, statsmodels 0.14.4) and JMP Pro 18.0.2 software. All experiments were independently replicated a minimum of three times unless stated otherwise, and each replicate represented an independent biological group (e.g., cage or clutch). The number of individuals or replicates used for each analysis is indicated in the figure panels and methods sections.

## Figure Legends

**Figure 1. Transgenic constructs and marker expression in *OpIE2a* and *OpIE2b* promoters driving A)** Transgenic construct design carrying either *OpIE2a*, *OpIE2b*, or *Actin5C* promoters driving DsRed, with or without a *U6*-sgRNA cassette. All were flanked by *piggyBac* inverted repeats and *attB* recombination sites enabling *φC31*-mediated site-specific integration. The genomic location and female blood-feeding phenotype are summarized on the right. **B)** Brightfield and fluorescence of fourth-instar larvae and pupae expressing DsRed under the *OpIE2a* promoter. **C)** Alignment of the *OpIE2a* and *OpIE2b* promoter sequences relative to the *Orgyia pseudotsugata* immediate early-2 (*IE-2*) gene. Both promoters share a common 461 bp core region, but *OpIE2a* extends 66 bp into the *IE-2* coding sequence, while *OpIE2b* includes an additional 90 bp upstream region and terminates before the start codon. **D)** Brightfield and fluorescence of fourth-instar larvae and pupae expressing DsRed under the *OpIE2b* promoter.

**Figure 2. Blood-feeding behavior of *OpIE2*-DsRed females**. **A)** Illustration of the experimental setup for the blood-feeding assay. Females were placed in minicages containing a camera and light source. A membrane-feeder filled with bovine blood was placed on top of the cage at the beginning of the experiment. **B–C)** Feeding success of wild type, *OpIE2b* and *OpIE2a* females. *OpIE2b*-DsRed females fed normally, whereas *OpIE2a*-DsRed females failed to feed. (**C**) Re-exposure of *OpIE2a*-DsRed females to a new feeder following 15min of resting with human-breath stimulation induced only occasional feeding. Boxplots show medians ± IQR; points represent independent replicate cages. N indicates the total number of females tested per treatment. Statistical significance was derived from unpaired two-sided *t*-tests, assuming equal or unequal variances, comparing the feeding rates between the different strains to the wild-type control ($\alpha = 0.05$). **D)** Feeder occupancy over time quantified by a YOLO-based behavioral tracking network. Solid lines show Gaussian-smoothed mean visits per minute ± SEM across (shaded ribbon) replicate cages. Statistical differences were assessed using a linear mixed-effects model with strain and time as fixed effects and replicate cage as a random intercept. *OpIE2a*-DsRed females spent significantly less time on the membrane-feeder and their visits declined rapidly compared to WT and *OpIE2b*-DsRed controls. **E)** Manually annotated behavioral ethograms during the first five minutes of the blood-feeding assay: Bars represent sequential visits by individual females, color-coded as on-feeder (gray), probing (blue), and blood-feeding (red). *OpIE2a*-DsRed females displayed repeated short probing attempts without transition to sustained feeding.

**Figure 3. Proboscis morphology and DsRed fluorescence in *Anopheles gambiae* adults carrying *OpIE2*-driven markers. (A–C)** Females and **(D–F)** males from wild-type (WT), *OpIE2b*-DsRed, and *OpIE2a*-DsRed strains imaged under bright-field (left) and fluorescence (middle, grayscale; right, red channel) illumination. **(A,D)** WT adults display a straight proboscis with no fluorescence. **(B,E)** *OpIE2b*-DsRed adults show strong, widespread DsRed expression but retain normal proboscis morphology. **(C,F)** *OpIE2a*-DsRed adults exhibit a pronounced distal curvature of the proboscis and strong DsRed signal localized on the proboscis and maxillary palps. Images were acquired under identical exposure settings to permit direct comparison of fluorescence intensity and anatomical deformation across strains and sexes.

**Figure 4. Reproductive output and fitness of *OpIE2*-DsRed strains. A–B)** Reproductive performance of females that successfully blood-fed. (**A**) Number of eggs laid per female and (**B**) corresponding hatching rate (% L1 per egg batch). Each point represents an individual female; Boxplots show medians ± IQR; N indicates the total number of eggs and hatched larvae tested per female. Statistical significance was derived from unpaired two-sided *t*-tests, assuming equal or unequal variances, comparing the feeding rates between the different strains to the wild-type control ($\alpha = 0.05$). *OpIE2a*-DsRed females produced significantly fewer eggs than wild-type (WT) or *OpIE2b*-DsRed females, while hatching rates did not differ significantly. **C–F)** Fitness parameters from crosses of transgenic males to WT females. (**C**) Hatching rate (% L1 per egg batch), (**D**) larval-to-pupal survival (%) and (**E**) pupal-to-adult survival (%) were comparable across strains. Boxplots show medians ± IQR; points represent replicate cages. (**F**) Adult sex ratios of progeny from the same crosses. Stacked bars show the mean proportion of males and females. Statistical comparisons were calculated relative to WT control using unpaired two-sided *t*-tests; no significant differences were detected (all $p > 0.05$). (**G-H)** Adult longevity of males (**G**) and females (**H**). *OpIE2a*-DsRed males exhibited a markedly reduced lifespan compared to WT and *OpIE2b*-DsRed males, while females showed a moderate but significant reduction in survival. Survival curves were analyzed using Kaplan-Meier estimates and compared using log-rank statistics. Diamonds denote median survival per strain.

**Supplementary Table 1. Summary of transgenic strains data** This table lists all transgenic strains generated in this study, including their creation date, transformation method, construct backbone, and associated phenotypes. Each strain is identified by an internal strain name. Construct number refers to the numbering system used to distinguish transformation plasmids. Integration method indicates whether transformation occurred through random *piggyBac*-mediated transposition or *φC31*-mediated site-specific integration. The sgRNA linker sequence shows the 5′-3′ sgRNA space sequence cloned for each construct containing a *U6*-sgRNA cassette. Larval marker phenotype denotes the strength and consistency of DsRed fluorescence, while female blood-feeding behavior and male fertility summarize adult phenotypic outcomes for each line.

**Supplementary Table 2. Heritable disruption of blood-feeding by *Opie2a*-DsRed.** Daughters of the two *OpIE2a*-DsRed females that successfully fed after additional stimulation (**Figure 2C**) were tested for blood-feeding capacity using the same experimental setup as their mothers. Three replicate cages were established, each containing nine 5–7-day-old females previously mated to wild-type males. In all replicates, no females were observed with visibly blood-filled abdomens at the end of the feeding period, confirming complete penetrance and transmission of the non-feeding phenotype.

**Supplementary Table 3. Manually annotated behavioral metrics of membrane feeding assays.** Table contains data for manually scored behavioral data obtained from BORIS ethograms (see **Figure 2E**) for individual *An. gambiae* females of the indicated genotypes (*OpIE2a*-DsRed, *OpIE2b*-DsRed, or wild-type). Each row represents a single female visit. Behavioral events were recorded from 5-min video segments and include the number of grooming and probing events, total time spent in the area of interest (AOI) near the feeder, and total duration of blood-feeding. “Time at AOI” represents cumulative occupancy on the feeder, while “ROI before feeding” and associated probing metrics quantify pre-feeding activity. Frequencies are expressed as events per second or minute as indicated.

**Author contributions**

AS and PAP conceived and designed the study. AS, ESY, ESMK and LBL generated transgenic mosquito lines. AS performed behavioral, imaging, and fitness assays, and analyzed the data.

ARL helped with figure illustrations. ES-S and JB developed the trained behavioral detection and classification neural network. ESMK, ESY, and LBL assisted with mosquito genetic engineering. TP and GP contributed to adult proboscis imaging. PAP supervised the project, secured funding, and wrote the manuscript together with AS with input from all authors. All authors read and approved the final manuscript.

**Acknowledgements**

We would like to thank Daniella An Haber and Yael Arien for their valuable discussions and critical feedback and Gleb Ens, Ruth Shacham and Albert Nazarov for technical support.

**Funding**

This work was supported by research grants from the Gates Foundation (INV-004363 and INV-075374 to PAP) and the Israel Science Foundation (ISF) (2388/19 to PAP).

**Ethics**

All animals were handled in accordance and under the supervision of the ARO Institutional Animal Care and Use Committee approval number 2307-118-2-VOL-IL. All insect work was performed in facilities maintaining Arthropod Containment Level 2. This work received Institutional Approval and relevant authorizations from the Israel Ministry of Environmental Protection and Ministry of Agriculture (#31/2019).

**Competing interests**

The authors declare no competing interests.

**References**

Adolfi, A. et al. (2018) “Multi-tissue GAL4-mediated gene expression in all Anopheles gambiae life stages using an endogenous polyubiquitin promoter,” Insect Biochemistry and Molecular Biology, 96, pp. 1–9. Available at: https://doi.org/10.1016/j.ibmb.2018.03.005.

Adolfi, A. et al. (2019) “Functional genetic validation of key genes conferring insecticide resistance in the major African malaria vector, Anopheles gambiae,” Proceedings of the National Academy of Sciences of the United States of America, 116(51), pp. 25764–25772. Available at: https://doi.org/10.1073/pnas.1914633116.

Berghammer, A.J., Klingler, M. and Wimmer, E.A. (1999) “A universal marker for transgenic insects,” Nature, 402(6760), pp. 370–371. Available at: https://doi.org/10.1038/46463.

Buchman, A.B. et al. (2018) “Engineered Reciprocal Chromosome Translocations Drive High Threshold, Reversible Population Replacement in Drosophila,” ACS synthetic biology, 7(5), pp. 1359–1370. Available at: https://doi.org/10.1021/acssynbio.7b00451.

Carballar-Lejarazú, R. et al. (2020) “Next-generation gene drive for population modification of the malaria vector mosquito, Anopheles gambiae,” Proceedings of the National Academy of Sciences, 117(37), pp. 22805–22814. Available at: https://doi.org/10.1073/pnas.2010214117.

Catteruccia, F. et al. (2000) “Stable germline transformation of the malaria mosquito Anopheles stephensi,” Nature, 405(6789), pp. 959–962. Available at: https://doi.org/10.1038/35016096.

Catteruccia, F., Benton, J.P. and Crisanti, A. (2005) “An Anopheles transgenic sexing strain for vector control,” Nature Biotechnology, 23(11), pp. 1414–1417. Available at: https://doi.org/10.1038/nbt1152.

Catteruccia, F., Godfray, H.C.J. and Crisanti, A. (2003) “Impact of Genetic Manipulation on the Fitness of Anopheles stephensi Mosquitoes,” Science, 299(5610), pp. 1225–1227. Available at: https://doi.org/10.1126/science.1081453.

Champer, S.E. et al. (2022) “Anopheles homing suppression drive candidates exhibit unexpected performance differences in simulations with spatial structure,” eLife. Edited by G.H. Perry, S.A. Verkuijl, and J. Bull, 11, p. e79121. Available at: https://doi.org/10.7554/eLife.79121.

Davydova, S. et al. (2023) “Next-generation genetic sexing strain establishment in the agricultural pest Ceratitis capitata,” Scientific Reports, 13(1), p. 19866. Available at: https://doi.org/10.1038/s41598-023-47276-5.

Estevez-Castro, C.F. et al. (2024) “Neofunctionalization driven by positive selection led to the retention of the loqs2 gene encoding an Aedes specific dsRNA binding protein,” BMC Biology, 22, p. 14. Available at: https://doi.org/10.1186/s12915-024-01821-4.

Feng, X. et al. (2021) “Optimized CRISPR tools and site-directed transgenesis towards gene drive development in Culex quinquefasciatus mosquitoes,” Nature Communications, 12, p. 2960. Available at: https://doi.org/10.1038/s41467-021-23239-0.

Friard, O. and Gamba, M. (2016) “BORIS: A free, versatile open-source event-logging software for video/audio coding and live observations,” Methods in Ecology and Evolution, 7. Available at: https://doi.org/10.1111/2041-210X.12584.

Fu, G. et al. (2010) “Female-specific flightless phenotype for mosquito control,” Proceedings of the National Academy of Sciences, 107(10), pp. 4550–4554. Available at: https://doi.org/10.1073/pnas.1000251107.

Georgiades, M. et al. (2023) “Hearing of malaria mosquitoes is modulated by a beta-adrenergic-like octopamine receptor which serves as insecticide target,” Nature Communications, 14(1), p. 4338. Available at: https://doi.org/10.1038/s41467-023-40029-y.

Giraldo, D. et al. (2024) “An expanded neurogenetic toolkit to decode olfaction in the African malaria mosquito Anopheles gambiae,” Cell Reports Methods, 4(2), p. 100714. Available at: https://doi.org/10.1016/j.crmeth.2024.100714.

Grossman, G.L. et al. (2001) “Germline transformation of the malaria vector,Anopheles gambiae, with the piggyBac transposable element,” Insect Molecular Biology, 10(6), pp. 597–604. Available at: https://doi.org/10.1046/j.0962-1075.2001.00299.x.

Haber, D.A. et al. (2024) “Targeting mosquito X-chromosomes reveals complex transmission dynamics of sex ratio distorting gene drives,” Nature Communications, 15(1), p. 4983. Available at: https://doi.org/10.1038/s41467-024-49387-7.

Irvin, N. et al. (2004) “Assessing fitness costs for transgenic Aedes aegypti expressing the GFP marker and transposase genes,” Proceedings of the National Academy of Sciences, 101(3), pp. 891–896. Available at: https://doi.org/10.1073/pnas.0305511101.

Jones, J.C. (1978) “The Feeding Behavior of Mosquitoes,” Scientific American, 238(6), pp. 138–150.

Kandul, N.P. et al. (2019) “Transforming insect population control with precision guided sterile males with demonstration in flies,” Nature Communications, 10(1), p. 84. Available at: https://doi.org/10.1038/s41467-018-07964-7.

Khanam, R. and Hussain, M. (2024) “YOLOv11: An Overview of the Key Architectural Enhancements.” arXiv. Available at: https://doi.org/10.48550/arXiv.2410.17725.

Kong, X.Q. and Wu, C.W. (2010) “Mosquito proboscis: An elegant biomicroelectromechanical system,” Physical Review E, 82(1), p. 011910. Available at: https://doi.org/10.1103/PhysRevE.82.011910.

Kyrou, K. et al. (2018) “A CRISPR–Cas9 gene drive targeting doublesex causes complete population suppression in caged Anopheles gambiae mosquitoes,” Nature Biotechnology, 36(11), pp. 1062–1066. Available at: https://doi.org/10.1038/nbt.4245.

Li, M. et al. (2017) “Germline Cas9 expression yields highly efficient genome engineering in a major worldwide disease vector, Aedes aegypti,” Proceedings of the National Academy of Sciences, 114(49), pp. E10540–E10549. Available at: https://doi.org/10.1073/pnas.1711538114.

Li, Z. et al. (2015) “Enhancement of Larval RNAi Efficiency by Over-expressing Argonaute2 in Bombyx mori,” International Journal of Biological Sciences, 11(2), pp. 176–185. Available at: https://doi.org/10.7150/ijbs.10235.

Li, Z. et al. (2025) “Driving a protective allele of the mosquito FREP1 gene to combat malaria,” Nature, pp. 1–9. Available at: https://doi.org/10.1038/s41586-025-09283-6.

Liu, J. et al. (2025) “Fluorescent-Based Sex-Separation Technique in Major Invasive Crop Pest, Drosophila suzukii,” GEN Biotechnology, 4(1), pp. 29–36. Available at: https://doi.org/10.1089/genbio.2024.0056.

Liu, J., Rayes, D. and Akbari, O.S. (2024) “A Fluorescent Sex-Sorting Technique for Insects with the Demonstration in Drosophila melanogaster,” GEN biotechnology, 3(1), pp. 35–44. Available at: https://doi.org/10.1089/genbio.2023.0041.

Lutrat, C. et al. (2022) “Transgenic expression of Nix converts genetic females into males and allows automated sex sorting in Aedes albopictus,” Communications Biology, 5(1), p. 210. Available at: https://doi.org/10.1038/s42003-022-03165-7.

Lycett, G.J., Amenya, D. and Lynd, A. (2012) “The Anopheles gambiae alpha-tubulin-1b promoter directs neuronal, testes and developing imaginal tissue specific expression and is a sensitive enhancer detector,” Insect Molecular Biology, 21(1), pp. 79–88. Available at: https://doi.org/10.1111/j.1365-2583.2011.01112.x.

Maguire, S.E. et al. (2022) “Odorant-receptor-mediated regulation of chemosensory gene expression in the malaria mosquito Anopheles gambiae,” Cell Reports, 38(10), p. 110494. Available at: https://doi.org/10.1016/j.celrep.2022.110494.

Marois, E. (2024) “Sorting Mosquito Larvae with a COPAS Machine,” Cold Spring Harbor Protocols, 2024(6), p. pdb.prot108307. Available at: https://doi.org/10.1101/pdb.prot108307.

Marrelli, M.T. et al. (2006) “Mosquito transgenesis: what is the fitness cost?,” Trends in Parasitology, 22(5), pp. 197–202. Available at: https://doi.org/10.1016/j.pt.2006.03.004.

Martins, S. et al. (2012) “Germline transformation of the diamondback moth, Plutella xylostella L., using the piggyBac transposable element,” Insect Molecular Biology, 21(4), pp. 414–421. Available at: https://doi.org/10.1111/j.1365-2583.2012.01146.x.

McArthur, C.C., Meredith, J.M. and Eggleston, P. (2014) “Transgenic Anopheles gambiae Expressing an Antimalarial Peptide Suffer No Significant Fitness Cost,” PLOS ONE, 9(2), p. e88625. Available at: https://doi.org/10.1371/journal.pone.0088625.

Meredith, J.M. et al. (2011) “Site-Specific Integration and Expression of an Anti-Malarial Gene in Transgenic Anopheles gambiae Significantly Reduces Plasmodium Infections,” PLOS ONE, 6(1), p. e14587. Available at: https://doi.org/10.1371/journal.pone.0014587.

Meredith, J.M. et al. (2013) “Next-Generation Site-Directed Transgenesis in the Malaria Vector Mosquito Anopheles gambiae: Self-Docking Strains Expressing Germline-Specific phiC31 Integrase,” PLoS ONE, 8(3), p. e59264. Available at: https://doi.org/10.1371/journal.pone.0059264.

Papathanos, P.A. et al. (2009) “The vasa regulatory region mediates germline expression and maternal transmission of proteins in the malaria mosquito Anopheles gambiae: a versatile tool for genetic control strategies,” BMC Molecular Biology, 10(1), p. 65. Available at: https://doi.org/10.1186/1471-2199-10-65.

Pascini, T.V. et al. (2022) “Transgenic Anopheles mosquitoes expressing human PAI-1 impair malaria transmission,” Nature Communications, 13(1), pp. 1–16. Available at: https://doi.org/10.1038/s41467-022-30606-y.

Pfeifer, T.A. et al. (1997) “Baculovirus immediate-early promoter-mediated expression of the ZeocinTM resistance gene for use as a dominant selectable marker in Dipteran and Lepidopteran insect cell lines,” Gene, 188(2), pp. 183–190. Available at: https://doi.org/10.1016/S0378-1119(96)00756-1.

Riabinina, O. et al. (2016) “Organization of olfactory centres in the malaria mosquito Anopheles gambiae,” Nature Communications, 7(1), p. 13010. Available at: https://doi.org/10.1038/ncomms13010.

Rouyar, A. et al. (2024) “Transgenic line for characterizing GABA-receptor expression to study the neural basis of olfaction in the yellow-fever mosquito,” Frontiers in Physiology, 15, p. 1381164. Available at: https://doi.org/10.3389/fphys.2024.1381164.

Scali, C. et al. (2005) “Identification of sex-specific transcripts of the Anopheles gambiae doublesex gene,” Journal of Experimental Biology, 208(19), pp. 3701–3709. Available at: https://doi.org/10.1242/jeb.01819.

Simmons, G.S. et al. (2011) “Field Performance of a Genetically Engineered Strain of Pink Bollworm,” PLoS ONE, 6(9), p. e24110. Available at: https://doi.org/10.1371/journal.pone.0024110.

Spinner, S.A.M. et al. (2022) “New self-sexing Aedes aegypti strain eliminates barriers to scalable and sustainable vector control for governments and communities in dengue-prone environments,” Frontiers in Bioengineering and Biotechnology, 10. Available at: https://doi.org/10.3389/fbioe.2022.975786.

Strampelli, A. et al. (2025) “A male-drive female-sterile system for the self-limited control of the malaria mosquito Anopheles gambiae.” bioRxiv, p. 2025.06.10.658817. Available at: https://doi.org/10.1101/2025.06.10.658817.

Tang, X.-F. et al. (2018) “Bombyx mori cyclin-dependent kinase inhibitor is involved in regulation of the silkworm cell cycle,” Insect Molecular Biology, 27(3), pp. 404–413. Available at: https://doi.org/10.1111/imb.12381.

Theilmann, D.A. and Stewart, S. (1992) “Molecular analysis of the trans-activating IE-2 gene of Orgyia pseudotsugata multicapsid nuclear polyhedrosis virus,” Virology, 187(1), pp. 84–96. Available at: https://doi.org/10.1016/0042-6822(92)90297-3.

Tolosana, I. et al. (2025) “A Y chromosome-linked genome editor for efficient population suppression in the malaria vector Anopheles gambiae,” Nature Communications, 16(1), p. 206. Available at: https://doi.org/10.1038/s41467-024-55391-8.

Vainer, Y. et al. (2024) “A conserved odorant receptor underpins borneol-mediated repellency in culicine mosquitoes,” bioRxiv, p. 2023.08.01.548337. Available at: https://doi.org/10.1101/2023.08.01.548337.

Verkuijl, S.A.N. et al. (2025) “A suppression-modification gene drive for malaria control targeting the ultra-conserved RNA gene mir-184,” Nature Communications, 16(1), p. 3923. Available at: https://doi.org/10.1038/s41467-025-58954-5.

Volohonsky, G. et al. (2015) “Tools for Anopheles gambiae Transgenesis,” G3: Genes|Genomes|Genetics, 5(6), pp. 1151–1163. Available at: https://doi.org/10.1534/g3.115.016808.

Weng, S.-C. et al. (2023) “Efficient sex separation by exploiting differential alternative splicing of a dominant marker in Aedes aegypti,” PLoS genetics, 19(11), p. e1011065. Available at: https://doi.org/10.1371/journal.pgen.1011065.

Weng, S.-C. et al. (2024) “Establishing a dominant early larval sex-selection strain in the Asian malaria vector Anopheles stephensi,” Infectious Diseases of Poverty, 13(1), p. 83. Available at: https://doi.org/10.1186/s40249-024-01256-7.

Witherbee, A.D. and Gamez, S. (2025) “Dissecting the sterility phenotype in gene edited Drosophila suzukii pgSIT males,” Scientific Reports, 15, p. 3903. Available at: https://doi.org/10.1038/s41598-025-88598-w.

Xu, J. et al. (2013) “Soaking RNAi-mediated modification of Sf9 cells for baculovirus expression system by ectopic expression of Caenorhabditis elegans SID-1,” Applied Microbiology and Biotechnology, 97(13), pp. 5921–5931. Available at: https://doi.org/10.1007/s00253-013-4785-1.

Zaada, D.S. et al. (2025) “Mosquito Sex Separation using Complementation of Selectable Traits and Engineered Neo-Sex Chromosomes.” bioRxiv, p. 2025.03.30.646185. Available at: https://doi.org/10.1101/2025.03.30.646185.

# Figure 1

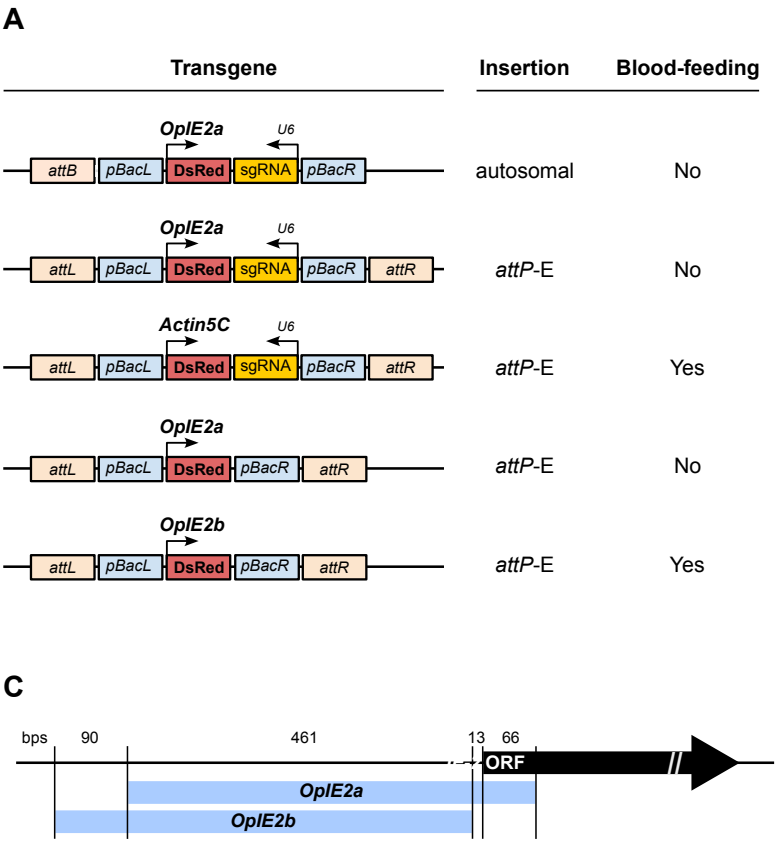
A
Transgene
Insertion
Blood-feeding
OpIE2a
U6
attB
pBacL
DsRed
sgRNA
pBacR
autosomal
No
OpIE2a
U6
attL
pBacL
DsRed
sgRNA
pBacR
attR
attP-E
No
Actin5C
U6
attL
pBacL
DsRed
sgRNA
pBacR
attR
attP-E
Yes
OpIE2a
attL
pBacL
DsRed
pBacR
attR
attP-E
No
OpIE2b
attL
pBacL
DsRed
pBacR
attR
attP-E
Yes
C
bps
90
461
13
66
ORF
OpIE2a
OpIE2b

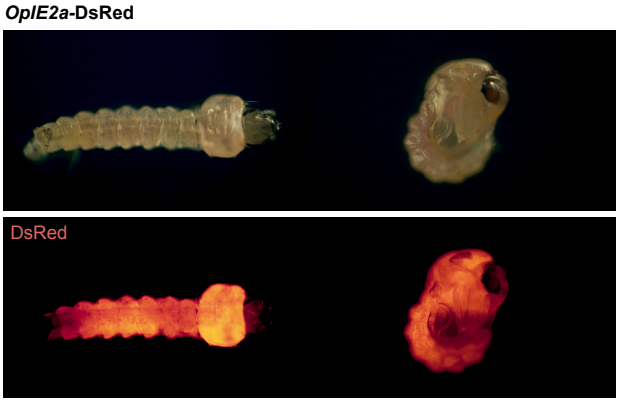
B
OpIE2a-DsRed
DsRed

D
OpIE2b-DsRed
DsRed

# Figure 2

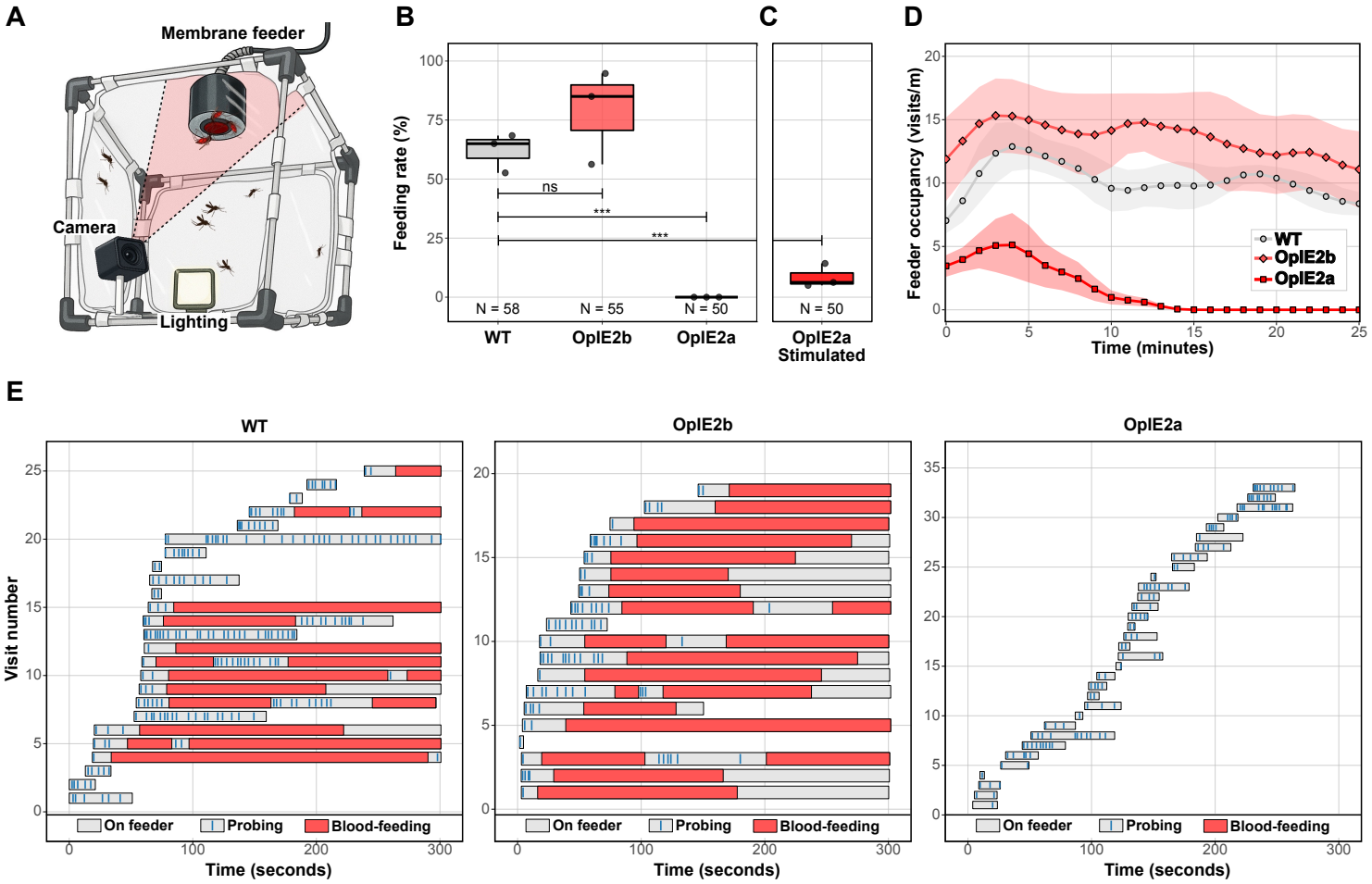
A
Membrane feeder
Camera
Lighting
B
Feeding rate (%)
ns
***
***
N = 58
N = 55
N = 50
WT
OpIE2b
OpIE2a
C
N = 50
OpIE2a
Stimulated
D
Feeder occupancy (visits/m)
Time (minutes)
WT
OpIE2b
OpIE2a
E
WT
OpIE2b
OpIE2a
Visit number
Time (seconds)
On feeder
Probing
Blood-feeding

# Figure 3

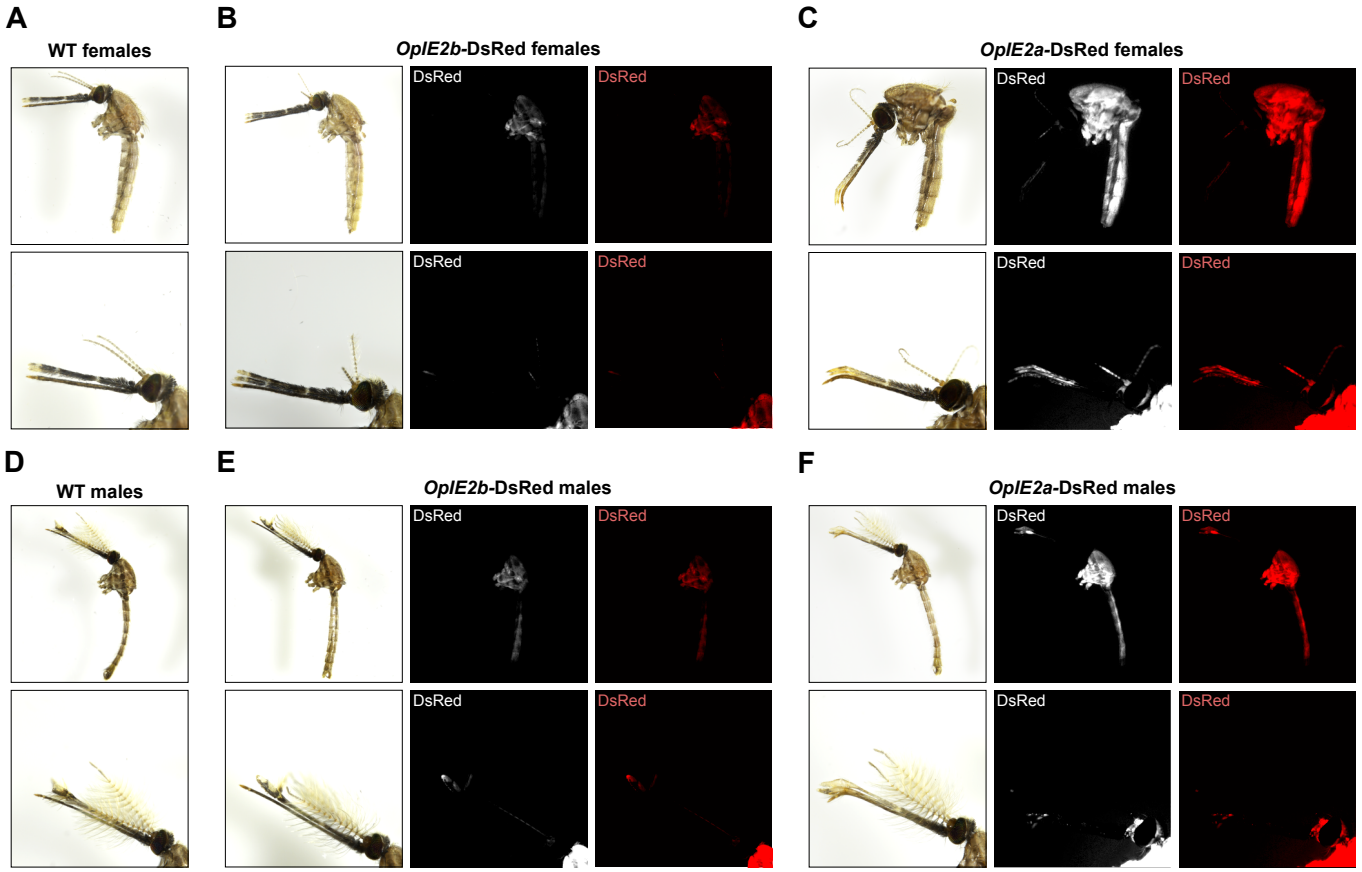
A
WT females
B
*OpIE2b*-DsRed females
DsRed
DsRed
DsRed
DsRed
C
*OpIE2a*-DsRed females
DsRed
DsRed
DsRed
DsRed
D
WT males
E
*OpIE2b*-DsRed males
DsRed
DsRed
DsRed
DsRed
F
*OpIE2a*-DsRed males
DsRed
DsRed
DsRed
DsRed

# Figure 4

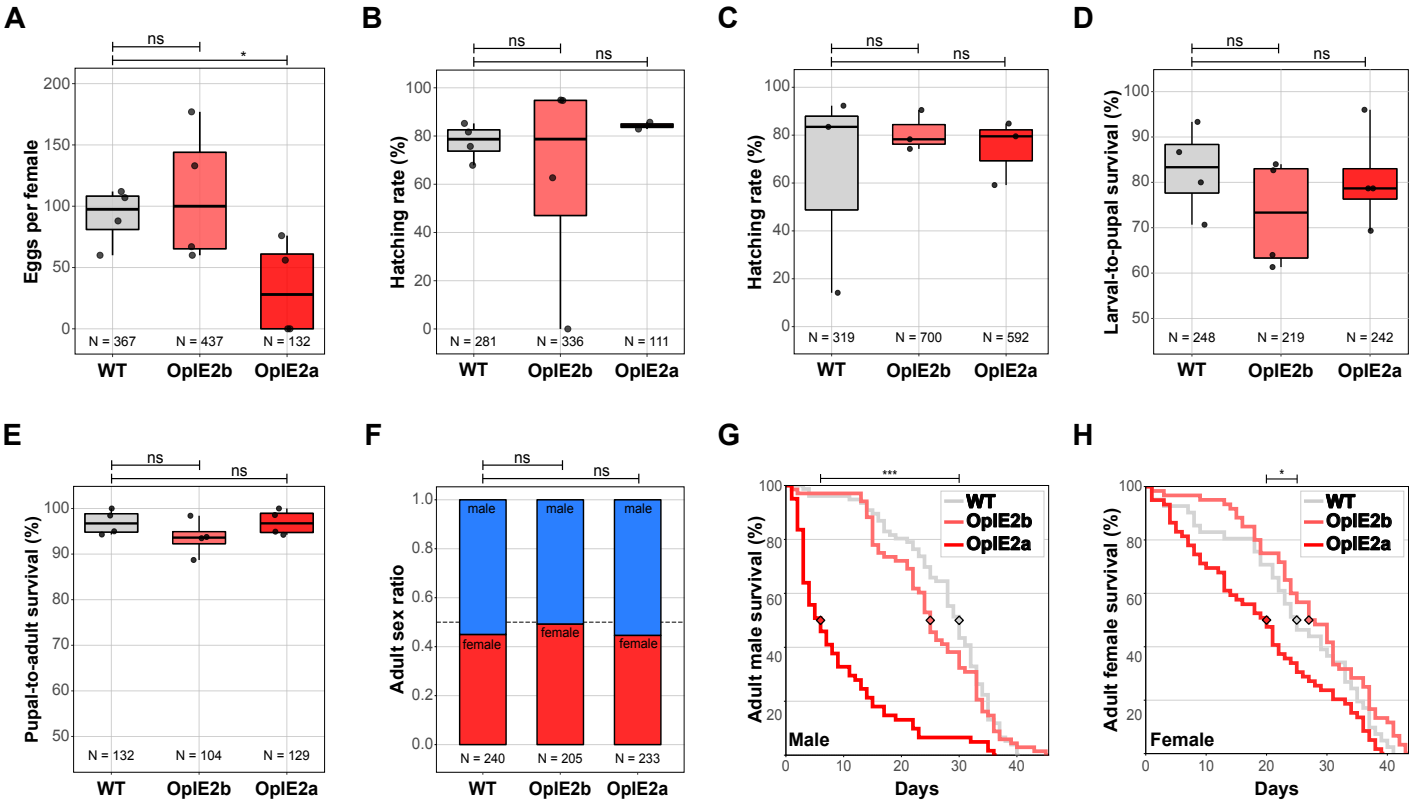
A
Eggs per female
ns
*
N = 367
N = 437
N = 132
WT
OpIE2b
OpIE2a
B
Hatching rate (%)
ns
ns
N = 281
N = 336
N = 111
C
Hatching rate (%)
ns
ns
N = 319
N = 700
N = 592
D
Larval-to-pupal survival (%)
ns
ns
N = 248
N = 219
N = 242
E
Pupal-to-adult survival (%)
ns
ns
N = 132
N = 104
N = 129
F
Adult sex ratio
ns
ns
male
female
N = 240
N = 205
N = 233
G
Adult male survival (%)
***
WT
OpIE2b
OpIE2a
Male
Days
H
Adult female survival (%)
*
WT
OpIE2b
OpIE2a
Female
Days